arXiv:1411.4153v2 [math.AP] 26 Nov 2014

PETVIASHVILLI'S METHOD FOR THE DIRICHLET PROBLEM

D. OLSON*, S. SHUKLA*, G. SIMPSON†, AND D. SPIRN*

Abstract. We examine the Petviashvilli method for solving the equation $\phi - \Delta\phi = |\phi|^{p-1}\phi$ on a bounded domain $\Omega \subset \mathbb{R}^d$ with Dirichlet boundary conditions. We prove a local convergence result, using spectral analysis, akin to the result for the problem on $\mathbb{R}$ by Pelinovsky & Stepanyants [16]. We also prove a global convergence result by generating a suite of nonlinear inequalities for the iteration sequence, and we show that the sequence has a natural energy that decreases along the sequence.

1. Introduction. Many nonlinear dispersive wave equations, including the nonlinear Schrödinger equation (NLS)

$$iu_t + \Delta u + |u|^{p-1}\, u = 0, \quad u : \mathbb{R}^{d+1} \to \mathbb{C}, \tag{1.1}$$

and the nonlinear wave equation (NLW)

$$u_{tt} = \Delta u + |u|^{p-1}\, u, \quad u : \mathbb{R}^{d+1} \to \mathbb{C}. \tag{1.2}$$

possess exact nonlinear bound state solutions, such as solitons. These can be obtained by first making the ansatz $u(x,t) = e^{i\lambda t}\phi(x)$ with $\lambda \in \mathbb{R}$. For (1.1), one obtains

$$-\lambda\phi + \Delta\phi + |\phi|^{p-1}\,\phi = 0, \quad \phi : \mathbb{R}^d \to \mathbb{C}. \tag{1.3}$$

A similar equation is obtained for (1.2), but with λ^2 in place of λ. Typically, we also assume

$$\lim_{|x|\to\infty} |\phi(x)| = 0, \tag{1.4}$$

though other boundary conditions are possible. A challenge to computing numerical solutions to (1.3) such that (1.4) holds is that $\phi = 0$ is a solution. Indeed, one could attempt to solve (1.3) by discretizing it and then applying Newton's method. But its success would depend on the initial guess, u_0, which could be in the domain of attraction of the zero solution. Thus, there is demand for an algorithm which can avoid the trivial solution without requiring preconditioning of a starting guess.

The same concerns arise when we consider the prototypical semilinear elliptic equation

$$-\phi + \Delta\phi + |\phi|^{p-1}\,\phi = 0, \quad \phi : \Omega \to \mathbb{R} \tag{1.5}$$

$$\phi|_{\partial\Omega} = 0, \tag{1.6}$$

where Ω is a bounded subset of $\mathbb{R}^d$ with sufficiently smooth boundary. This problem appears when one tries to numerically solve (1.3) subject to (1.4). First the problem must be reformulated on a finite domain, Ω, and then an artificial boundary condition must be introduced. Here, we consider the Dirichlet boundary condition, (1.6). Inspired by work on (1.3) in [17], we shall adapt and analyze Petviashvilli's method, discussed below, to the Dirichlet problem.

*SCHOOL OF MATHEMATICS, UNIVERSITY OF MINNESOTA, MINNEAPOLIS, MN 55455, USA

†DEPARTMENT OF MATHEMATICS, DREXEL UNIVERSITY, PHILADELPHIA, PA 19104, USA

1.1. Ground States and Excited States. Associated with (1.5) is the energy functional

$$E(\psi) := \frac{1}{2}\|\psi\|_{H^1}^2 - \frac{1}{p+1}\|\psi\|_{L^{p+1}}^{p+1}. \tag{1.7}$$

Taking the first variation of (1.7), we see that critical points of E correspond to weak solutions, in the sense of H^1, of (1.5). In general, this functional is unbounded from below, so solutions of (1.5) do not correspond to global minimizers. However, if one considers the question of minimizing the energy over the set of nontrivial solutions to (1.5), one finds that there is indeed a minimizer—the so called ground state [4,6,20].

In general, one cannot rule out the existence of other nontrivial solutions to (1.5). Indeed, we immediately have that if u is a solution, so is $-u$. But more complicated solutions may also arise. For the problem posed on all of $\mathbb{R}^d$, there are infinitely many other solutions [20]. As these have greater energy than the ground state, they are deemed to be excited states.

Here, we will develop an algorithm which may be of use in computing both ground and excited state solutions.

1.2. Petviashvilli's Method & Related Algorithms. Originally developed to obtain soliton solutions of a Kadomtsev–Petviashvilli equation, Petviashvilli's iteration method for (1.5) is

$$u_{n+1} = M[u_n]^\gamma (I-\Delta)^{-1}\left(|u_n|^{p-1}u_n\right), \tag{1.8a}$$

$$M[u] = \frac{\langle (I-\Delta)u, u\rangle}{\left\langle |u|^{p-1}u, u\right\rangle}, \tag{1.8b}$$

where the inner product is that of L^2, and γ is in an admissible range identified below in Assumption 3. For brevity of notation, we denote the iteration operator for (1.8) by $\mathcal{A}$:

$$u_{n+1} = \mathcal{A}(u_n).$$

As was shown in [16], this method is locally non-linearly convergent about non-linear bound states. There, the result was demonstrated for the case of $d = 1$ and on the real line but allowed for more general elliptic operators. Analysis of the algorithm to more specific cases appeared in [7] for a fifth order Korteweg–de Vries equation and in [8] for cubic NLS in $\mathbb{R}^3$. In practice, this algorithm is extremely robust to the choice of u_0. Initial conditions, far from any solution, still converge to solutions of (1.5); see the numerical experiments, below, in Section 5. This robustness, which is not addressed by local analysis, is one of the main motivations for our work.

Petviashvilli's method was also generalized in [12,15] allowing for external potentials and more complicated (*i.e.* non-homogeneous) nonlinearities. In these works, they were able to handle semilinear elliptic systems and also obtained excited state solutions. The performance of the algorithm was also improved using "mode elimination" [13]. More recently, the M functional, (1.8b), was generalized in [3].

Algorithms related to Petviashvilli's method include the imaginary time method [22], the squared operator method [21], and spectral renormalization [1]. The imaginary time method allows the user to find a solution of (1.3) with a given L^2 norm, but unknown constant λ. This if of use in certain physical applications such as Bose-Einstein condensate. The squared operator method improves the performance and

stability of these algorithms. Lastly, spectral renormalization allows for more general nonlinearities and external potentials.

Numerically, solutions are typically sought for the problem posed on $\mathbb{R}$ or $\mathbb{R}^2$ by studying the problem on a sufficiently large finite domain, $[-x_{\max}, x_{\max})^d$, with periodic boundary conditions. This allows for the use of the Fast Fourier Transform, making the inversion of constant coefficient elliptic operators easy. In at least one work, where a radially symmetric solution was sought, the domain was reduced to $[0, \infty)$, and an artificial Robin boundary condition was imposed at some $r_{\max}$ [5].

1.3. Main Results & Relations to Other Work. We consider the Dirichlet problem, (1.5), and apply iteration scheme (1.8) to obtain non-trivial solutions. In this context, we are able to obtain a strong local convergence result and a weak global convergence result.

For both results, we make the following assumptions:

ASSUMPTION 1. *$\Omega \subset \mathbb{R}^d$ is a bounded, convex, open set (hence, it has Lipschitz boundary).*

ASSUMPTION 2. *The nonlinearity is superlinear and subcritical, satisfying:*

$$1 < p < d^\dagger \equiv \begin{cases} \infty & d = 1, 2, \\ \frac{d+2}{d-2} & d \geq 3. \end{cases} \tag{1.9}$$

Next, we assume that γ lives in an admissible range, identified in [16],

ASSUMPTION 3.

$$1 < \gamma < \frac{p+1}{p-1}. \tag{1.10}$$

Assumption 1 is essential to our use of elliptic theory and Sobolev embedding results. For computation, this is a very mild restriction, as our domains are typically polygonal or smoother. Assumption 2 is needed to ensure the existence of non-trivial solutions to (1.5) and will be used throughout the paper. Assumption 3 is needed for the algorithm to be linearly stable. Within the range of admissible γ, a distinguished value is

$$\gamma_\star = \frac{p}{p-1}. \tag{1.11}$$

This will play a special role in both our linear and nonlinear analysis.

To state our first result, we will need one additional, spectral, assumption. We note here, and highlight again in Section 2.2, that p is an eigenvalue of $(I-\Delta)^{-1}(p\,|\phi|^{p-1}\,\bullet)$ corresponding to the eigenfunction ϕ. We assume:

ASSUMPTION 4. *Viewing $(I-\Delta)^{-1}(p\,|\phi|^{p-1}\,\bullet)$ as an operator from H_0^1 to itself,*

$$\sigma((I-\Delta)^{-1}(p\,|\phi|^{p-1}\,\bullet)) \setminus (-\infty, 1) = \{p\}\,, \tag{1.12}$$

and the algebraic multiplicity of p is one.

Our first result is on the local convergence of the algorithm.

THEOREM 1.1 (Strong Local Convergence). *Assume Assumptions 1, 2, 3, and 4 hold. Given a solution ϕ of (1.5), let $\mathcal{A}'(\phi) : H_0^1(\Omega) \to H_0^1(\Omega)$ denote the linearization of (1.8) about ϕ.*

There exists a neighborhood, $\mathcal{N}$, of ϕ in H_0^1 and a constant $\theta \in (0,1)$ such that for all $u_0 \in \mathcal{N}$, the sequence of iterates, $\{u_n\}_{n=0}^\infty$, defined through (1.8) satisfies

$$\|u_n - \phi\|_{H^1} \leq \theta^n \|u_0 - \phi\|_{H^1}\,.$$

Our second main result is:

THEOREM 1.2 (Subsequential Global Convergence).

Assume Assumptions 1 and 2 hold and that u_0 is any nontrivial H_0^1 function. Also assume that $\gamma = \gamma_\star$, defined in (1.11).

Let $\{u_n\}_{n=0}^{\infty}$ be a sequence of functions generated by (1.8).

- *Assume $d \geq 2$. There exists a subsequence $\{u_{n_k}\}$ that converges strongly in H_0^1 to a nontrivial strong solution of* (1.5) *in $W^{2,2}$ for $d = 2$ and to a strong solution in $W^{2,\kappa}$ for $d \geq 3$ where $\kappa = \min\left\{2, \frac{2^*}{p}\right\}$. The Sobolev conjugate, 2^*, is defined as $2^* = \frac{2d}{d-2}$.*
- *Assume either $d = 1$ or $d \geq 2$ with $\partial\Omega$ is smooth. Then, for all $\ell \in 2\mathbb{Z}^+$, there exists a strongly convergent subsequence in C^ℓ, and its limit, $\phi \in C^\infty$, is a nontrivial solution of* (1.5).

Combining these two results, we have:

COROLLARY 1.3. *If the limit obtained in Theorem 1.2 satisfies Assumption 4, then the entire sequence converges to ϕ.*

Thus, we have a partial answer towards the question of the robustness of the algorithm with respect ot the choice of u_0.

The proof of Theorem 1.1 is based on the result in [16] for the problem on $\mathbb{R}$. See [7, 8, 12] for related analysis of the algorithm. Theorem 1.2 is proven by compactness methods, and we believe it to be novel.

1.4. Outline. Our paper is organized as follows. In Section 2, we review some preliminary results on the existence and regularity of nonlinear bound states, the well-posedness of the iteration scheme, and important spectral properties of the iteration operator. In Section 3, we prove Theorem 1.1, and a proof of Theorem 1.2 is given in Section 4. Example computations appear in Section 5 followed by a discussion in Section 6.

2. Preliminary Results. In this section, we provide some definitions, review some properties of the bound states, and examine the iteration scheme. For brevity, we define

$$\mathcal{L} \equiv I - \Delta.$$

As an inner product on $H_0^1(\Omega)$, we use

$$\langle f, g \rangle_{H^1} = \langle \mathcal{L}f, g \rangle = \langle f, \mathcal{L}g \rangle = \int_\Omega fg + \nabla f \cdot \nabla g.$$

Weak solutions of (1.5) are functions, $\phi \in H_0^1(\Omega)$ such that for all $v \in H_0^1$,

$$\int_\Omega \nabla\phi \cdot \nabla v + \phi v + |\phi|^{p-1}\phi v = 0$$

Relating this to the iteration scheme, we have the following elementary result:

LEMMA 2.1. *If $u \in H_0^1$ is a fixed point of* (1.8) *and $M[u] = 1$, then u is a weak solution of* (1.5).

Proof. Since $\mathcal{L} : H_0^1 \to H^{-1}$ has trivial kernel, $\mathcal{L}$ can be applied to both sides of (1.8) to obtain $\mathcal{L}u = |u|^{p-1}u$, with equality holding in H^{-1}. □

Existence of weak, nontrivial solutions subject to Assumptions 1 and 2 is well established and can be found in, for example, [4, 6]. If we assume that $\partial\Omega$ is C^∞, then, using bootstrap methods and elliptic regularity theory, ϕ will also be smooth.

2.1. Properties of the Iteration Method. Before proceeding with an analysis of the algorithm, we need to establish certain properties.

PROPOSITION 2.2. *Assume Assumptions 1 and 2 hold. If $u \in H_0^1$ and $u \neq 0$, then $\mathcal{A}(u) \in H_0^1$ and $\mathcal{A}(u) \neq 0$.*

Proof. By the standard Sobolev embeddings, since $u \in H_0^1$, $u \in L^{p+1}$. Therefore the numerator and denominator of $M[u]$ are both finite. In addition, since $u \neq 0$, the denominator is nonzero. Hence, $M[u]$ is well defined. Next, observe that $|u|^{p-1} u \in H^{-1}$. Finally, we have that $\mathcal{L}^{-1}(|u|^{p-1} u) \in H_0^1$; hence, $\mathcal{A}(u) \in H_0^1$. Since $M[u] > 0$, we must have that $\mathcal{A}(u) \neq 0$. ∎

This implies that the iteration scheme is well defined in the sense that, though $\|u_n\|_{H^1}$ could tend to infinity as $n \to \infty$, $u_{n+1} \in H_0^1$ can always be computed from u_n.

PROPOSITION 2.3. *Assume Assumptions 1 and 2 hold and that $\gamma > 1$. Then about any $u \in H_0^1$, $u \neq 0$:*

- *$\mathcal{A}$ is continuous;*
- *$\mathcal{A}$ is Fréchet differentiable;*
- *The Fréchet derivative, $\mathcal{A}'(\bullet) : H_0^1 \to L(H_0^1)$, is continuous with respect to the H^1 operator norm.*

The Fréchet derivative is given by:

$$\mathcal{A}'(u)h = M[u]^\gamma \mathcal{L}^{-1}(p\,|u|^{p-1} h) + \gamma \frac{[M'[u], h]}{M[u]} \mathcal{A}(u),$$

$$[M'[u], h] = \frac{1}{\|u\|_{L^{p+1}}^{p+1}} \left[2\,\langle u, h \rangle_{H^1} - (p+1) M[u] \left\langle |u|^{p-1} u, h \right\rangle \right].$$

Proof. The proof of this is standard, and, for brevity, we omit it. ∎

2.2. Spectral Results. At a nontrivial solution ϕ of (1.5), $M[\phi] = 1$, $\mathcal{L}\phi = |\phi|^{p-1} \phi$, and $\mathcal{A}(\phi) = \phi$. Therefore the linearization at ϕ simplifies to:

$$\mathcal{A}'(\phi)h = \mathcal{L}^{-1}(p\,|\phi|^{p-1} h) - \gamma(p-1) \frac{\langle \phi, h \rangle_{H^1}}{\langle \phi, \phi \rangle_{H^1}} \phi. \tag{2.2}$$

Equation (2.2) is quite informative as to the local behavior of the algorithm. Returning to (1.5), one might ask why not apply the iteration scheme

$$u_{n+1} = \mathcal{L}^{-1}(|u_n|^{p-1} u_n). \tag{2.3}$$

Linearizing (2.3) about ϕ, we obtain

$$\mathcal{L}^{-1}(p\,|\phi|^{p-1} h),$$

which is the first term in (2.2). Observe that this has an eigenvalue with modulus in excess of unity:

$$\mathcal{L}^{-1}(p\,|\phi|^{p-1} \phi) = p\phi.$$

Thus, there is a linearly unstable mode, and (2.3) will diverge. In (2.2), a rank one orthogonal projection is added, shifting the unstable eigenvalue into the interior of the unit disk. Indeed,

$$\mathcal{A}'(\phi)\phi = p\phi - \gamma(p-1)\phi = (p - \gamma(p-1))\,\phi. \tag{2.4}$$

Assumption 3 is precisely what ensures that the eigenvalue corresponding to ϕ lies in the interval $-1 < p - \gamma(p-1) < 1$.

Next, we have:

PROPOSITION 2.4. *$\mathcal{L}^{-1}(p\,|\phi|^{p-1}\,\bullet) : H_0^1 \to H_0^1$ is compact.*

Proof. Given any bounded sequence $\{u_n\}$ in H_0^1, it contains a weakly convergent subsequence, $\{u_{n_k}\}$, with limit $u \in H_0^1$. Thus, to show that the operator is compact, it suffices to show that it maps weakly convergent H^1 sequences to strongly convergent ones. Consider the case of $d \geq 3$, as $d = 1, 2$ are simpler. First, we have

$$\begin{aligned}
&\left\|\mathcal{L}^{-1}(p\,|\phi|^{p-1}\,(u_{n_k} - u))\right\|_{H^1}^2 = \left\langle \mathcal{L}^{-1}(p\,|\phi|^{p-1}\,(u_{n_k} - u)), (p\,|\phi|^{p-1}\,(u_{n_k} - u))\right\rangle \\
&\leq \left\|\mathcal{L}^{-1}(p\,|\phi|^{p-1}\,(u_{n_k} - u))\right\|_{L^{2^*}} \left\|p\,|\phi|^{p-1}\right\|_{L^{\frac{2^*}{p-1}}} \|u_{n_k} - u\|_{L^{\frac{2^*}{2^*-p}}}.
\end{aligned}$$

Since H^1 continuously embeds into L^{2^*} and $L^{\frac{2^*}{p-1}}$, the first two norms in the above expression are controlled by H^1. Next, since p is subcritical, satisfying (1.9), we have that $2^*/(2^* - p) < 2^*$; therefore,

$$\left\|\mathcal{L}^{-1}(p\,|\phi|^{p-1}\,(u_{n_k} - u))\right\|_{H^1} \leq C\,\|u_{n_k} - u\|_{L^{\frac{2^*}{2^*-p}}}.$$

By Rellich, the subsequence converges strongly in the $L^{\frac{2^*}{2^*-p}}$ topology, and we have the desired convergence. □

We can now summarize the spectrum of the operator $\mathcal{L}^{-1}(p\,|\phi|^{p-1}\,\bullet)$:

THEOREM 2.5 (Spectrum of $\mathcal{L}^{-1}(p\,|\phi|^{p-1}\,\bullet)$).

1. *$\mathcal{L}^{-1}(p\,|\phi|^{p-1}\,\bullet)$ is self-adjoint with respect to the H^1 inner product and the spectrum is real.*
2. *$\mathcal{L}^{-1}(p\,|\phi|^{p-1}\,\bullet) : H_0^1 \to H_0^1$ has a complete orthonormal basis, $\{\psi_j\}$, with $\mathcal{L}^{-1}(p\,|\phi|^{p-1}\,\psi_j) = \nu_j\psi_j$ and $\nu_j \to 0$ and $\nu_j \geq 0$.*
3. *$\mathcal{L}^{-1}(p\,|\phi|^{p-1}\,\phi) = p\phi$.*

Proof. Self-adjointness follows by inspection, and this immediately implies that the spectrum must be real. Since it is compact on H_0^1 and self-adjoint on the separable Hilbert space H_0^1, it has a complete orthonormal basis, and all nonzero eigenvalues have finite multiplicity; see Theorems VI.15 and VI.16 of [18]. As previously noted, p is an eigenvalue with ϕ the corresponding eigenfunction. Lastly, given any ν_j, we compute,

$$\nu_j = \nu_j \langle \psi_j, \psi_j \rangle_{H^1} = \left\langle \mathcal{L}^{-1}(p\,|\phi|^{p-1}\,\psi_j), \psi_j \right\rangle_{H^1} = \left\langle p\,|\phi|^{p-1}\,\psi_j, \psi_j \right\rangle \geq 0.$$

□

We then immediately obtain results on the spectrum of $\mathcal{A}'(\phi)\bullet$:

COROLLARY 2.6. *$\mathcal{A}'(\phi)\bullet : H_0^1 \to H_0^1$ is a compact.*

Proof. Since $\mathcal{A}'(\phi)\bullet$ is a compact operator plus rank one operator, it is compact.

□

COROLLARY 2.7 (Spectrum of $\mathcal{A}'(\phi)$).

1. *$\mathcal{A}'(\phi)\bullet$ is self adjoint with respect to the H^1 inner product, and the spectrum of $\mathcal{A}'(\phi)\bullet$ is real.*
2. *$\mathcal{A}'(\phi)\bullet : H_0^1 \to H_0^1$ has a complete orthonormal basis, $\{\psi_j\}$, with $\mathcal{A}'(\phi)\psi_j = \mu_j\psi_j$ and $\mu_j \to 0$.*
3. *$\mathcal{A}'(\phi)\phi = (p - (p-1)\gamma)\phi$.*

4. For all $\mu_j \neq p-(p-1)\gamma$, $\mu_j \geq 0$.

Assumption 4 thus ensures that p is the only linearly unstable mode of $\mathcal{L}^{-1}(p\,|\phi|^{p-1}\,\bullet)$, which is linearly stable for $\mathcal{A}'(\phi)\bullet$.

Proof. All of this follows from the last corollary and Theorem 2.5. The eigenvalues ν_j and μ_j relate to one another as

$$\mu_j = \begin{cases} \nu_j, & \nu_j \neq p, \\ p-(p-1)\gamma, & \nu_j = p. \end{cases}$$

This follows from $\mathcal{A}'(\phi)\bullet$ being a rank one perturbation, where the rank one term is an orthogonal spectral projection.
∎

3. Local Convergence. Given $v_0 \in H^1_0$, let v_n denote the sequence generated by the linearized operator:

$$v_{n+1} = \mathcal{A}'(\phi)v_n. \tag{3.1}$$

First, we decompose the iterates.

PROPOSITION 3.1. *The sequence v_n can be decomposed as $v_n = a_n\phi + w_n$, where $w_n \perp_{H^1} \phi = 0$, and a_n and w_n satisfy the decoupled equations:*

$$w_{n+1} = \mathcal{L}^{-1}(p\,|\phi|^{p-1}\,w_n) \tag{3.2a}$$
$$a_{n+1} = (p-\gamma(p-1))a_n. \tag{3.2b}$$

REMARK 3.2. *Notice in the case that $\gamma = \gamma_\star = \frac{p}{p-1}$, (3.2b) implies that $a_n = 0$ for all $n \geq 1$, regardless of the choice of a_0.*

Proof. This follows from the spectral decomposition of the operator. Indeed, at any iterate, we can define

$$a_n = \frac{\langle \phi, v_n\rangle_{H^1}}{\langle \phi, \phi\rangle_{H^1}}$$

and then let $w_n = v_n - a_n\phi$. Thus, $w_n \perp_{H^1} \phi$. Comparing sequential iterates, we see

$$\begin{aligned} v_{n+1} = \mathcal{A}'(\phi)v_n &= \mathcal{A}'(\phi)w_n + a_n\mathcal{A}'(\phi)\phi, \\ w_{n+1} + a_{n+1}\phi &= \mathcal{L}^{-1}(p\,|\phi|^{p-1}\,w_n) + (p-\gamma(p-1))a_n\phi. \end{aligned}$$

Taking the H^1 inner product of both sides with ϕ, we have $a_{n+1} = (p-\gamma(p-1))a_n$. Going back and cancelling this out in the equation above yields $w_{n+1} = \mathcal{L}^{-1}(p\,|\phi|^{p-1}\,w_n)$.
∎

PROPOSITION 3.3. *Assuming that Assumptions 1,2, 3, and 4 hold, let*

$$\mu_\star = \sup \sigma(\mathcal{L}^{-1}(p\,|\phi|^{p-1}\,\bullet)) \setminus \{p\}\,.$$

Then $\mu_\star \in [0,1)$, and for sequence (3.1)

$$\|v_n\|_{H^1} \leq \max\{|p-\gamma(p-1)|\,, \mu_\star\}^n \|v_0\|_{H^1}\,. \tag{3.3}$$

REMARK 3.4. *Again, $\gamma = \gamma_\star$ plays a distinguished role in the above contraction estimate, making the constant $\mu_\star^n$.*

Proof. By virtue of spectral assumption (1.12) and the compactness of $\mathcal{L}^{-1}(p\,|\phi|^{p-1}\,\bullet)$, we are assured that $\mu_\star < 1$. This is because the only possible cluster point in the spectrum of a compact operator is zero. The fact that $\mu_\star \geq 0$ follows from Theorem 2.5.

Writing $v_{n+1} = w_{n+1} + a_{n+1}\phi$ and recalling $w_n \perp_{H^1} \phi$,

$$\begin{aligned}\|v_{n+1}\|_{H^1}^2 &= \|w_{n+1}\|_{H^1}^2 + 2a_{n+1}\langle w_{n+1}, \phi\rangle_{H^1} + a_{n+1}^2\|\phi\|_{H^1}^2 \\ &= \|w_{n+1}\|_{H^1}^2 + a_{n+1}^2\|\phi\|_{H^1}^2 .\end{aligned}$$

Since $w_n \perp_{H^1} \phi$ and since we have assumed p is the only eigenvalue of $\mathcal{L}^{-1}(p\,|\phi|^{p-1}\,\cdot)$ greater than or equal to one, then, by the spectral decomposition of the operator,

$$w_{n+1} = \mathcal{L}^{-1}(p\,|\phi|^{p-1}\,w_n) = \sum_{\mu_j<1} \mu_j\,\langle\psi_j, w_{n+1}\rangle_{H^1}\,\psi_j.$$

Therefore,

$$\|w_{n+1}\|_{H^1}^2 = \sum_{\mu_j<1} |\mu_j|^2\,\left|\langle\psi_j, w_{n+1}\rangle_{H^1}\right|^2 \leq \mu_\star^2\,\|w_{n+1}\|_{H^1}^2 ,$$

and

$$\begin{aligned}\|v_{n+1}\|_{H^1}^2 &\leq \mu_\star^2\,\|w_{n+1}\|_{H^1}^2 + |p-\gamma(p-1)|^2\,a_n^2\,\|\phi\|_{H^1}^2 \\ &\leq \max\left\{\mu_\star^2, |p-\gamma(p-1)|^2\right\}\|v_n\|_{H^1}^2 .\end{aligned}$$

□

Finally, we state our local nonlinear convergence result.

THEOREM 3.5. *Under the same assumptions as in Proposition 3.3, further assume γ satisfies* (1.10)*. Then there exists a neighborhood $\mathcal{N}$ of ϕ such that if $u_0 \in \mathcal{N}$, then $u_n \to \phi$.*

Proof. Let $\eta = \max\{|p-\gamma(p-1)|, \mu_\star\} < 1$. Since $u \mapsto \mathcal{A}'(u)$ is continuous in the operator norm (see Proposition 2.3), there is a neighborhood $\mathcal{N}$ of ϕ, such that

$$\sup_{u\in\mathcal{N}}\|\mathcal{A}'(u)\| \leq \sup_{u\in\mathcal{N}}\|\mathcal{A}'(u)-\mathcal{A}'(\phi)\| + \|\mathcal{A}'(\phi)\| \leq \frac{1}{2}(1-\eta)+\eta = \frac{1+\eta}{2} < 1.$$

Let $\theta \equiv (1+\eta)/2$. By the mean value theorem for Fréchet differentiable functions, [11], for all $u, v \in \mathcal{N}$,

$$\|\mathcal{A}(u)-\mathcal{A}(v)\|_{H^1} \leq \sup_{w\in\mathcal{N}}\|\mathcal{A}'(w)\|\,\|u-v\|_{H^1} \leq \theta\,\|u-v\|_{H^1} .$$

Therefore, we have a contraction, with parameter θ.
□

4. Global Convergence. In this section we provide results concerning the global convergence of $\{u_n\}$ and prove Theorem 1.2.

4.1. Nonlinear Estimates. Before we can proceed, we need certain *a priori* estimates on our sequence. We emphasize that these estimates are inherently nonlinear, in contrast to those used to prove Theorem 1.1. We also define the α exponent,

$$\alpha \equiv \gamma - \gamma p + p, \tag{4.1}$$

which will play an important role in what follows. By Assumptions 2 and 3, we are assured that $|\alpha| < 1$.

First, we have the following sequential inequalities.

LEMMA 4.1. *Assume Assumptions 1, 2, and 3 hold. Also assume that $u_0 \in H^1$ is nontrivial. Then the following identities hold for the sequence generated by* (1.8) *for all $n \geq 0$:*

$$M[u_n]^{\gamma-1} \leq \frac{\|u_{n+1}\|_{H^1}}{\|u_n\|_{H^1}}, \tag{4.2a}$$

$$\frac{\|u_{n+1}\|_{H^1}}{\|u_{n+1}\|_{L^{p+1}}} \leq \frac{\|u_n\|_{H^1}}{\|u_n\|_{L^{p+1}}}, \tag{4.2b}$$

$$M[u_n]^{\gamma-1} \geq \frac{\|u_{n+1}\|_{H^1}^2}{\|u_n\|_{H^1}^2} \frac{\|u_n\|_{L^{p+1}}}{\|u_{n+1}\|_{L^{p+1}}}, \tag{4.2c}$$

$$M[u_{n+1}] \leq M[u_n]^{\alpha}, \tag{4.2d}$$

with α defined as in (4.1).

Proof. **Step 1.** Applying $I - \Delta$ to both sides of (1.8), we have

$$(I - \Delta)u_{n+1} = M[u_n]^{\gamma}(|u_n|^{p-1}u_n). \tag{4.3}$$

Multiplying by u_n and integrating by parts, we obtain the discrete identity

$$\frac{\langle u_{n+1}, u_n \rangle_{H^1}}{\|u_n\|_{H^1}^2} = M[u_n]^{\gamma-1}. \tag{4.4}$$

Applying Cauchy-Schwarz to the above expression, we have (4.2a).

Step 2. If we multiply (4.3) by u_{n+1}, integrate by parts, and then use Hölder's inequality we have

$$\|u_{n+1}\|_{H^1}^2 \leq M[u_n]^{\gamma} \|u_{n+1}\|_{L^{p+1}} \|u_n\|_{L^{p+1}}^p. \tag{4.5}$$

On the other hand, if we multiply (4.3) by u_n and use Cauchy-Schwarz on the H^1 inner product, we have

$$M[u_n]^{\gamma} \|u_n\|_{L^{p+1}}^{p+1} \leq \|u_{n+1}\|_{H^1} \|u_n\|_{H^1}. \tag{4.6}$$

Next, multiplying (4.5) by $\|u_n\|_{L^{p+1}}$ and using (4.6), we have

$$\|u_{n+1}\|_{H^1}^2 \|u_n\|_{L^{p+1}} \leq M[u_n]^{\gamma} \|u_n\|_{L^{p+1}}^{p+1} \|u_{n+1}\|_{L^{p+1}} \leq \|u_{n+1}\|_{H^1} \|u_n\|_{H^1} \|u_{n+1}\|_{L^{p+1}}.$$

Inductively applying Proposition 2.2, we are assured that u_n is always nontrivial, so we can divide both sides of the above expression by $\|u_{n+1}\|_{H^1} \|u_{n+1}\|_{L^{p+1}} \|u_n\|_{L^{p+1}}$ to get, by induction,

$$\frac{\|u_{n+1}\|_{H^1}}{\|u_{n+1}\|_{L^{p+1}}} \leq \frac{\|u_n\|_{H^1}}{\|u_n\|_{L^{p+1}}} \leq \cdots \leq \frac{\|u_0\|_{H^1}}{\|u_0\|_{L^{p+1}}} \equiv C_0. \tag{4.7}$$

This is (4.2b), and we have a reverse Sobolev embedding along the sequence

$$\|u_n\|_{H^1} \leq C_0 \|u_n\|_{L^{p+1}}. \tag{4.8}$$

Recall the standard Sobolev embedding

$$\|u_n\|_{L^{p+1}} \leq C_p \|u_n\|_{H^1}, \tag{4.9}$$

for all $n \geq 0$ since $p < d^\dagger$.

Step 3. To establish (4.2d), we first note

$$\frac{M[u_{n+1}]}{M[u_n]} = \frac{\|u_{n+1}\|_{H^1}^2}{\|u_n\|_{H^1}^2} \frac{\|u_n\|_{L^{p+1}}^{p+1}}{\|u_{n+1}\|_{L^{p+1}}^{p+1}} \overset{(4.7)}{\leq} \frac{\|u_n\|_{L^{p+1}}^{p-1}}{\|u_{n+1}\|_{L^{p+1}}^{p-1}},$$

so

$$\frac{\|u_n\|_{L^{p+1}}}{\|u_{n+1}\|_{L^{p+1}}} \geq \left(\frac{M[u_{n+1}]}{M[u_n]}\right)^{\frac{1}{p-1}}. \tag{4.10}$$

Next, squaring (4.6) and dividing by $\|u_{n+1}\|_{L^{p+1}}^{p+1} \|u_n\|_{H^1}^2$, we get

$$\begin{aligned} M[u_{n+1}] &\geq M[u_n]^{2\gamma} \frac{\|u_n\|_{L^{p+1}}^{p+1}}{\|u_n\|_{H^1}^2} \frac{\|u_n\|_{L^{p+1}}^{p+1}}{\|u_{n+1}\|_{L^{p+1}}^{p+1}} \\ &= M[u_n]^{2\gamma-1} \frac{\|u_n\|_{L^{p+1}}^{p+1}}{\|u_{n+1}\|_{L^{p+1}}^{p+1}} \overset{(4.10)}{\geq} M[u_n]^{2\gamma-1} \frac{M[u_{n+1}]^{\frac{p+1}{p-1}}}{M[u_n]^{\frac{p+1}{p-1}}}, \end{aligned}$$

so

$$M[u_{n+1}]^{\frac{-2}{p-1}} \geq M[u_n]^{\frac{(2\gamma-1)(p-1)-p-1}{p-1}} = M[u_n]^{\frac{-2\alpha}{p-1}},$$

yielding (4.2d).

□

REMARK 4.2. *In the case that $\gamma = \gamma_\star = \frac{p}{p-1}$ (and $\alpha = 0$), we immediately have that $M[\phi_n] \leq 1$ for all $n \geq 1$. Thus, $\gamma_\star$ plays a distinguished role in both the linear and nonlinear analysis of the problem.*

Using this result, we can obtain the following estimates on the entire sequence. The main tools are the following uniform estimates for the sequence of solutions.

PROPOSITION 4.3. *Assume Assumptions 1, 2, and 3 hold. Let u_n be a sequence generated via* (1.8) *with nontrivial u_0.*

- *There exist positive constants C_1 and C_2 depending only on Ω, d, γ, p, $\|u_0\|_{H^1}$, and $\|u_0\|_{L^{p+1}}$ such that for all $n \geq 0$,*

$$0 < C_1 \leq \|u_n\|_{H^1} \leq C_2. \tag{4.11}$$

.

- *There exists a positive constant C_3 (with the same dependencies as C_1 and C_2) such that for all $n \geq 1$,*

$$C_3 \geq \begin{cases} \|u_n\|_{W^{2,2}} & d = 2, \\ \|u_n\|_{W^{2,\kappa}} & d \geq 3, \kappa = \min\left\{\frac{2^*}{p}, 2\right\}. \end{cases} \tag{4.12}$$

- *If either $\partial\Omega$ is smooth or $d = 1$, then there exists $k_0 \in \mathbb{N}$, depending only on d and p, such that for all $n \geq n_0$, $u_n \in C^{2(n-n_0)}$.*

The proof of the proposition relies on the regularity of weak solutions to the elliptic equation $(I - \Delta)v = f$. We state these classical L^q regularity results in the following two lemmas for future reference. The first addresses the situation of a smooth boundary and can be found in, e.g., Theorems 9.13 and 9.15 of [10]. The second concerns the case of a convex domain. It is a slight variant of Corollary 1 of [9]; see also [2].

LEMMA 4.4. *Let $\Omega \subset \mathbb{R}^d$ be an open, bounded set, and assume that either $d = 1$ or $\partial\Omega$ is smooth. Let $f \in L^q(\Omega)$ for some $1 < q < \infty$. Then the equation $(I-\Delta)v = f$ in Ω with $v = 0$ on $\partial\Omega$ has a unique weak solution $v \in W^{2,q}(\Omega)$ satisfying the estimate*

$$\|v\|_{W^{2,q}(\Omega)} \leq C\big(\|f\|_{L^q(\Omega)} + \|v\|_{L^q(\Omega)}\big). \tag{4.13}$$

LEMMA 4.5. *Let $f \in L^q(\Omega) \cap H^{-1}(\Omega)$ for some $1 < q \leq 2$, and assume that $d \geq 2$ with Ω satisfying Assumption 1. Let $v \in H_0^1(\Omega)$ be the unique weak solution to $(I - \Delta)v = f$ in Ω with $v = 0$ on $\partial\Omega$, and further assume that $v \in L^q(\Omega)$. Then $v \in W^{2,q}(\Omega)$, and*

$$\|v\|_{W^{2,q}(\Omega)} \leq C\big(\|f\|_{L^q(\Omega)} + \|v\|_{L^q(\Omega)}\big). \tag{4.14}$$

Proof. [Proof of Proposition 4.3]

To establish the regularity of the sequence we use the estimates generated from Lemma 4.1. In the following, we focus on $d \geq 3$. The cases $d = 1, 2$ are somewhat simpler.

Step 1. We first consider the growth of the H^1-norms of the u_n's generated by the iteration:

$$\begin{aligned}\|u_{n+1}\|_{H^1} &\overset{(4.5),(4.9)}{\leq} C_p M[u_n]^\gamma \|u_n\|_{L^{p+1}}^p = C_p \|u_n\|_{H^1}^{2\gamma} \|u_n\|_{L^{p+1}}^{p-(p+1)\gamma} \\ &\overset{(4.8),(4.9)}{\leq} C_p^{p+1} C_0^{\gamma(p+1)} \|u_n\|_{H^1}^{\gamma-\gamma p+p}.\end{aligned}$$

Thus,

$$\|u_{n+1}\|_{H^1} \leq A \|u_n\|_{H^1}^\alpha, \tag{4.15}$$

where we have taken

$$A = \max\{C_p^{p+1} C_0^{\gamma(p+1)}, 1\}.$$

Likewise, (4.6), (4.8), and (4.9) imply the lower bound

$$\|u_{n+1}\|_{H^1} \geq B \|u_n\|_{H^1}^\alpha, \tag{4.16}$$

where we have set

$$B = \min\{C_p^{-\gamma(p+1)} C_0^{-p-1}, 1\}.$$

Step 2. Note that (4.11) holds trivially when $\alpha = 0$. Now consider $0 < \alpha < 1$. By iterating, and using that $A \geq 1$,

$$\|u_n\|_{H^1} \leq A^{\sum_{k=0}^{n-1} \alpha^k} \|u_0\|_{H^1}^{\alpha^n} \leq A^{\frac{1}{1-\alpha}} \|u_0\|_{H^1}^{\alpha^n}.$$

Similarly, since $B \le 1$ we have

$$\|u_n\|_{H^1} \ge B^{\sum_{j=0}^{n-1}\alpha^j} \|u_0\|_{H^1}^{\alpha^n} \ge B^{\frac{1}{1-\alpha}} \|u_0\|_{H^1}^{\alpha^n}.$$

Next, consider $-1 < \alpha < 0$. Using both (4.15) and (4.16), we find that

$$\left(\frac{B}{A^{|\alpha|}}\right) \|u_{n-2}\|_{H^1}^{|\alpha|^2} \le \|u_n\|_{H^1} \le \left(\frac{A}{B^{|\alpha|}}\right) \|u_{n-2}\|_{H^1}^{|\alpha|^2}.$$

Again, by iteration,

$$\|u_n\|_{H^1} \le \begin{cases} \left(\frac{A}{B^{|\alpha|}}\right)^{\frac{1}{1-|\alpha|^2}} \|u_0\|_{H^1}^{|\alpha|^n} & n \text{ even}, \\ \left(\frac{A}{B^{|\alpha|}}\right)^{\frac{1}{1-|\alpha|^2}} A^{|\alpha|^{n-1}} \|u_0\|_{H^1}^{-|\alpha|^n} & n \text{ odd}, \end{cases}$$

and

$$\|u_n\|_{H^1} \ge \begin{cases} \left(\frac{B}{A^{|\alpha|}}\right)^{\frac{1}{1-|\alpha|^2}} \|u_0\|_{H^1}^{|\alpha|^n} & n \text{ even}, \\ \left(\frac{B}{A^{|\alpha|}}\right)^{\frac{1}{1-|\alpha|^2}} A^{|\alpha|^{n-1}} \|u_0\|_{H^1}^{-|\alpha|^n} & n \text{ odd}. \end{cases}$$

These estimates imply (4.11).

Step 3. We now prove (4.12) for $d \ge 3$. We recall that $\kappa = \min\left\{2, \frac{2^*}{p}\right\}$ and consider the two cases, $\kappa = 2$ or $\kappa = \frac{2^*}{p}$. First suppose that $\kappa = \frac{2^*}{p}$ so $\frac{2^*}{p} \le 2$.

Using the regularity result (4.14) with $v = u_{n+1}$, $f = M[u_n]^\gamma |u_n|^{p-1}u_n$, and $q = \frac{2^*}{p}$, we obtain

$$\begin{aligned} \|u_{n+1}\|_{W^{2,\frac{2^*}{p}}} &\le CM[u_n]^\gamma \left\| |u_n|^{p-1} u_n \right\|_{L^{\frac{2^*}{p}}} + C\|u_{n+1}\|_{L^{\frac{2^*}{p}}} \\ &= C\frac{\|u_n\|_{H^1}^{2\gamma}}{\|u_n\|_{L^{p+1}}^{\gamma(p+1)}} \|u_n\|_{L^{2^*}}^p + CC_p\|u_{n+1}\|_{H^1} \\ &\le \left(CC_{2^*}^p C_0^{\gamma(p+1)} + ACC_p\right) \|u_n\|_{H^1}^\alpha, \end{aligned}$$

where we have used the reverse Sobolev embedding (4.8), standard Sobolev embedding, and (4.15) in the final inequality. As $\|u_n\|_{H^1} \le C_2$ uniformly in n, the $W^{2,\frac{2^*}{p}}$ bound (4.12) follows.

Now assume that $\kappa = 2$ so that $2 \le \frac{2^*}{p}$. We may again invoke (4.14) with $q = 2$ to deduce

$$\begin{aligned} \|u_{n+1}\|_{W^{2,2}} &\le CM[u_n]^\gamma \left\| |u_n|^{p-1} u_n \right\|_{L^2} + C\|u_{n+1}\|_{L^2} \\ &\le CM[u_n]^\gamma \left\| |u_n|^{p-1} u_n \right\|_{L^{\frac{2^*}{p}}} + C\|u_{n+1}\|_{H^1}. \end{aligned}$$

Proceeding as in the previous case gives the desired result.

A similar argument (without needing separate cases) holds for $d = 2$.

Step 4. When the boundary is smooth, we can further iterate the algorithm and generate improved regularity. But first we prove two small claims to organize the argument. If $v \in L^s$ and $f \in L^q$ with $1 < s < q < \infty$ with $s < \frac{d}{2}$ and $(I - \Delta)v = f$ then

$$\|v\|_{L^{\frac{sd}{d-2s}}} \le C\left(\|v\|_{L^s} + \|f\|_{L^q}\right). \tag{4.17}$$

To show this we note that since the domain is compact, $\|f\|_{L^s} \leq C\|f\|_{L^q}$ with a constant C depending on Ω. Since the boundary is smooth, by (4.13) we have

$$\|v\|_{W^{2,s}} \leq C\left(\|v\|_{L^s} + \|f\|_{L^q}\right),$$

and Sobolev embedding implies (4.17).

Step 5. Next, we claim that if $v \in L^r$ and $f \in L^q$ with $1 < r < q < \infty$ and $(I - \Delta)v = f$ then either $v \in C^{0,\beta}$ for some $\beta \in (0, 1]$ or $v \in W^{2,q}$ with

$$\|v\|_{W^{2,q}} \leq C\left(\|v\|_{L^r} + \|f\|_{L^q}\right). \tag{4.18}$$

We can prove (4.18) by iterating. Set $r_0 = r$, and consider a sequence of iterates r_j such that $v \in W^{2,r_j}$ and defined as follows. If $r_j > \frac{d}{2}$, then $v \in C^{0,\beta}$ for some $0 < \beta \leq 1$ by Morrey's inequality, and the iteration terminates. On the other hand, if $r_j = \frac{d}{2}$, then $v \in L^s$ for all $s < \infty$. In particular, $v \in L^q$, so (4.13) implies $v \in W^{2,q}$, and the iteration stops. Finally, if $r_j < \frac{d}{2}$, then by Step 4, $v \in L^{\frac{r_j d}{d-2r_j}}$. If $\frac{r_j d}{d-2r_j} \geq q$, then $v \in L^q$, (4.13) implies $v \in W^{2,q}$, and the iteration halts. If $\frac{r_j d}{d-2r_j} < q$, then set $r_{j+1} = \frac{r_j d}{d-2r_j}$ and continue the iteration.

Step 6.

We claim that there exists $n_0 \in \mathbb{N}$ such that $u_{n_0} \in C^{0,\beta}$ for a $0 < \beta \leq 1$. Note that if $u_n \in W^{2,r_n}$ with $r_n > \frac{d}{2}$, then by Morrey's inequality, $u_n \in C^{0,\beta_n}$ for $\beta_n = 2 - \frac{d}{r_n}$; therefore, we will iterate the Petviashvilli algorithm until we reach an n such that $r_n > \frac{d}{2}$. In the following we will use (4.11) which implies

$$\|u_j\|_{L^{2^*}} \leq C \qquad \text{for all } j \in \mathbb{N}. \tag{4.19}$$

If $r_n < \frac{d}{2}$, then we claim that either $u_{n+1} \in C^{0,\beta}$ for some $0 < \beta \leq 1$ or $u_{n+1} \in W^{2,r_{n+1}}$ with

$$r_{n+1} = \frac{dr_n}{p(d - 2r_n)}. \tag{4.20}$$

First note that by Sobolev embedding $u_n \in L^{s_n}$ with $\frac{1}{s_n} = \frac{1}{r_n} - \frac{2}{d}$ so $|u_n|^{p-1}u_n \in L^{\frac{s_n}{p}}$. Therefore, if $\frac{s_n}{p} \leq 2^*$, then (4.19) implies $u_{n+1} \in L^{\frac{s_n}{p}}$, and we can use (4.13) with $q = \frac{s_n}{p}$ to see that $u_{n+1} \in W^{2,r_{n+1}}$. If $\frac{s_n}{p} > 2^*$, then we use Step 5, which implies either $u_{n+1} \in C^{0,\beta}$ for some $0 < \beta \leq 1$ or $u_{n+1} \in W^{2,r_{k+1}}$ in which case r_{k+1} satisfies (4.20). We note that (4.20) is an increasing sequence so long as $p < d^\dagger$. This iteration can be solved explicitly with $r_1 = \frac{2^*}{p}$:

$$r_n = \frac{2d(p-1)}{4p - p^n\left((d+2) - (d-2)p\right)}.$$

We now iterate the sequence until $r_{n_0} > \frac{d}{2}$ at which point $W^{2,r_{n_0}}$ embeds in a Hölder space.

If $r_n = \frac{d}{2}$, then $u_n \in L^s$ for all $s < \infty$. We take $s = \frac{2d}{p}$ so $|u_n|^{p-1}u_n \in L^{\frac{2d}{p}}$. Following a similar argument as above shows that $u_{n+1} \in W^{2,\frac{2d}{p}} \subset C^{0,\beta}$ for some $0 < \beta \leq 1$.

Finally, we can use classical Schauder estimates to show that $u_n \in C^{2(n-n_0),\beta}$ for all $n \geq n_0$.

□

4.2. Global Convergence. *Proof.* [Theorem 1.2]

First, we recall Lemma 4.1 which implies that if $\gamma = \frac{p}{p-1}$ then $\alpha = 0$ and $M[u_n] \leq 1$ for all $n \geq 1$.

Step 1. We will first show that

$$\lim_{n\to\infty} M[u_n] = 1. \tag{4.21}$$

By (4.2a), we have $M[u_n]^{\gamma-1} \leq \|u_{n+1}\|_{H^1}/\|u_n\|_{H^1}$ so that

$$M[u_n]^{\gamma-1} M[u_{n-1}]^{\gamma-1} \cdots M[u_0]^{\gamma-1} \leq \frac{\|u_{n+1}\|_{H^1}}{\|u_n\|_{H^1}} \frac{\|u_n\|_{H^1}}{\|u_{n-1}\|_{H^1}} \cdots \frac{\|u_1\|_{H^1}}{\|u_0\|_{H^1}}.$$

Rewriting this as

$$\left(\prod_{k=0}^{n} M[u_k]\right)^{\gamma-1} \leq \frac{\|u_{n+1}\|_{H^1}}{\|u_0\|_{H^1}},$$

we can, from (4.11), conclude that

$$\prod_{k=0}^{n} M[u_k] \leq \left(\frac{\|u_{n+1}\|_{H^1}}{\|u_0\|_{H^1}}\right)^{\frac{1}{\gamma-1}} \leq C. \tag{4.22}$$

We repeat this argument with the lower bound (4.2c). In particular we get

$$\begin{aligned} M[u_n]^{\gamma-1} \cdots M[u_0]^{\gamma-1} &\geq \frac{\|u_{n+1}\|_{H^1}^2}{\|u_n\|_{H^1}^2} \cdots \frac{\|u_1\|_{H^1}^2}{\|u_0\|_{H^1}^2} \frac{\|u_n\|_{L^{p+1}}}{\|u_{n+1}\|_{L^{p+1}}} \cdots \frac{\|u_0\|_{L^{p+1}}}{\|u_1\|_{L^{p+1}}} \\ &= \frac{\|u_{n+1}\|_{H^1}^2}{\|u_0\|_{H^1}^2} \frac{\|u_0\|_{L^{p+1}}}{\|u_{n+1}\|_{L^{p+1}}}. \end{aligned}$$

Using (4.11) and (4.2b), we have

$$\prod_{k=0}^{n} M[u_k] \geq \left(\frac{\|u_{n+1}\|_{H^1}^2}{\|u_0\|_{H^1}^2} \frac{\|u_0\|_{L^{p+1}}}{\|u_{n+1}\|_{L^{p+1}}}\right)^{\frac{1}{\gamma-1}} \geq C > 0. \tag{4.23}$$

Now consider the series $\sum_{k=1}^{\infty} \log M[u_k]$. Since $\log M[u_k] \leq 0$ by (4.2d) and since

$$\sum_{k=0}^{\infty} \log M[u_k] \geq \log C > -\infty$$

from (4.23), the series converges. Therefore, $\lim_{n\to\infty} \log M[u_n] = 0$. This implies (4.21).

Step 2. Next we show that $\|u_{n+1} - u_n\|_{H^1} = \mathrm{o}_n(1)$ for all $n \geq 1$. We begin with the estimate

$$M[u_n]^{\gamma-1} \overset{(4.2c)}{\geq} \frac{\|u_{n+1}\|_{H^1}^2}{\|u_n\|_{H^1}^2} \frac{\|u_n\|_{L^{p+1}}}{\|u_{n+1}\|_{L^{p+1}}} \overset{(4.10)}{\geq} \frac{\|u_{n+1}\|_{H^1}^2}{\|u_n\|_{H^1}^2} \left(\frac{M[u_{n+1}]}{M[u_n]}\right)^{\frac{1}{p-1}}.$$

From this we obtain

$$\|u_{n+1}\|_{H^1}^2 \leq M[u_n]^{\gamma-1} \left(\frac{M[u_{n+1}]}{M[u_n]}\right)^{\frac{1}{p-1}} \|u_n\|_{H^1}^2. \tag{4.24}$$

Therefore,

$$\begin{aligned}\|u_{n+1}-u_n\|_{H^1}^2 &= \|u_{n+1}\|_{H^1}^2+\|u_n\|_{H^1}^2-2\left(u_{n+1},u_n\right)\\ &\overset{(4.4)}{=} \|u_{n+1}\|_{H^1}^2+\|u_n\|_{H^1}^2-2M[u_n]^{\gamma-1}\|u_n\|_{H^1}^2\\ &\overset{(4.24)}{\leq} \|u_n\|_{H^1}^2\left[1-2M[u_n]^{\gamma-1}+M[u_n]^{\gamma-1}\left(\frac{M[u_{n+1}]}{M[u_n]}\right)^{\frac{1}{p-1}}\right]\\ &\overset{(4.11)}{\leq} C\left[1-2M[u_n]^{\gamma-1}+M[u_n]^{\gamma-1}\left(\frac{M[u_{n+1}]}{M[u_n]}\right)^{\frac{1}{p-1}}\right].\end{aligned}$$

Since $M[u_n]\to 1$, the right-hand side vanishes as $n\to\infty$.

Step 3. We claim that our iteration converges to a strong solution to (1.5). Again, we present the argument for $d\geq 2$. By Proposition 4.3, we know that our sequence $\{u_n\}$ is uniformly bounded in $W^{2,\kappa}$ (where κ is defined in Theorem 1.2) so we can extract a weakly convergent subsequence, $\{u_{n_k}\}$, in $W^{2,\kappa}$, with limit $\phi\in W^{2,\kappa}$. By Rellich, $W^{2,\kappa}$ is compactly embedded in H^1 so this subsequence will converge strongly to ϕ in H_0^1.

From Step 2, we also know that $u_{n_k+1}\to\phi$, strongly in H_0^1. For any $\psi\in H_0^1$,

$$\left\langle u_{n_k+1},\psi\right\rangle_{H^1}=M[u_{n_k}]^{\gamma}\left\langle |u_{n_k}|^{p-1}u_{n_k},\psi\right\rangle,$$

and from the strong H^1 convergence of $\{u_{n_k+1}\}$ and Step 1, we have

$$\begin{aligned}\left\langle u_{n_k+1},\psi\right\rangle_{H^1}&\to\left\langle\phi,\psi\right\rangle_{H^1},\\ M[u_{n_k}]^{\gamma}\left\langle |u_{n_k}|^{p-1}u_{n_k},\psi\right\rangle&\to\left\langle|\psi|^{p-1}\psi,\psi\right\rangle.\end{aligned}$$

Thus, the limit ϕ is a weak solution of (1.5). Finally, by (4.12) we get the improved regularity of ϕ.

Step 4. When $\partial\Omega$ is smooth, we claim that $u_n\to\phi$ in C^k and that ϕ is a C^∞ solution to (1.5). Since $u_n\in C^{k,\beta}$ for, say, $k\geq 3$, by the compact embedding of $C^{k,\beta}$ in C^k, there exists a subsequence $\{u_{n_k}\}\subset\{u_n\}$ and a limit $\phi\in C^k$ such that $u_{n_k}\to\phi$ strongly in C^k.

Now, from the iteration scheme,

$$u_{n_k+1}=(I-\Delta)^{-1}\left(M[u_{n_k}]^{\gamma}|u_{n_k}|^{p-1}u_{n_k}\right)$$

is a strongly convergent sequence in C^{k+2}. Therefore, $\{u_{n_k+1}\}$ is a Cauchy sequence in C^k with a limit $\overline{\phi}$. However, by Step 2, as n_k tends to infinity,

$$\left\|\phi-\overline{\phi}\right\|_{H^1}\leq\|\phi-u_{n_k}\|_{H^1}+\|u_{n_k}-u_{n_k+1}\|_{H^1}+\left\|u_{n_k+1}-\overline{\phi}\right\|_{H^1}$$

goes to zero. Therefore, $\overline{\phi}=\phi$. Returning to the scheme, we find $u_{n_k+1}\to\phi$ and

$$(I-\Delta)\phi=|\phi|^{p-1}\phi$$

since $M[u_n]\to 1$ for all n.

□

REMARK 4.6. *It is natural to ask whether the sequence generated by the Petviashvilli iteration is, in fact, Cauchy; however, we are unable to show this, unless the*

limit ϕ satisfies the assumptions of Theorem 1.1 (see Corollary 1.3). On the other hand, one can follow Step 3 of the proof of Theorem 1.2 and use induction to show for any fixed $\ell \in \mathbb{Z}^+$ that $u_{n_k+\ell}$ is a subsequence converging to ϕ.

In order to prove that a.e. sequence is Cauchy, it would be sufficient to show that $|1 - M[u_n]^{\gamma-1}| \leq Cn^{-\sigma}$ for some $\sigma > 1$.

Proof. [Corollary 1.3] If the subsequential limit, ϕ, satisfies the spectral condition, then Theorem 1.1 applies to it. Some element of the subsequence will be in the local basin of attraction of ϕ, and the linear theory implies the whole sequence converges to ϕ. □

4.3. Tendency to the Groundstate. As our numerical experiments show, (1.8) appears to always produce a ground state solution. Here, we provide some insight into this behavior. We first define a modified energy,

$$E_M[\psi] \equiv \begin{cases} \frac{1}{2}\|\psi\|_{H^1}^2 - \frac{1}{p+1}M[\psi]\|\psi\|_{L^{p+1}}^{p+1} & M[\psi] \leq 1, \\ +\infty & M[\psi] > 1. \end{cases}$$

In the case that $M[\psi] = 1$, we recover the standard energy $E_1[\psi] := E[\psi]$, as defined by (1.7).

We can rewrite $E_M[\psi]$ as

$$E_M[\psi] = \|\psi\|_{H^1}^2 \left[\frac{1}{2} - \frac{1}{p+1}\right]. \tag{4.25}$$

THEOREM 4.7. *Let u_n be an iteration generated by (1.8) with u_0 nontrivial initial data and $\gamma = \frac{p}{p-1}$. Then*

$$\liminf_{n\to\infty} E_1[u_n] \leq E_M[u_0]. \tag{4.26}$$

Given the solution ϕ extracted from Theorem 1.2, we possess

$$E_1[\phi] \leq E_M[u_0]. \tag{4.27}$$

The proof of Theorem 4.7 follows from Lemma 4.8 below.

LEMMA 4.8.

Assume that $\gamma = \gamma_\star = p/(p-1)$ and that

$$0 < M[u_k] \leq M[u_n] \leq 1 \tag{4.28}$$

for some $0 \leq k < n$. Then

$$E_M[u_n] \leq E_M[u_k],$$

with the inequality strict if $M[u_n] < M[u_k]$.

In particular, if $0 < M[u_k] \leq 1$, then

$$\liminf_{n\to\infty} E_1[u_n] \leq E_M[u_k].$$

Proof. We first obtain the estimate,

$$\frac{M[u_{n+1}]}{M[u_n]} = \frac{\|u_{n+1}\|_{H^1}^2}{\|u_n\|_{H^1}^2}\frac{\|u_n\|_{L^{p+1}}^{p+1}}{\|u_{n+1}\|_{L^{p+1}}^{p+1}} \leq \frac{\|u_n\|_{H^1}^{p-1}}{\|u_{n+1}\|_{H^1}^{p-1}} \Rightarrow \frac{\|u_{n+1}\|_{H^1}^2}{\|u_n\|_{H^1}^2} \leq \left(\frac{M[u_n]}{M[u_{n+1}]}\right)^{\frac{2}{p-1}}.$$

We now consider the telescoping product and use (4.25):

$$\frac{E_M[u_{n+1}]}{E_M[u_n]}\frac{E_M[u_n]}{E_M[u_{n-1}]}\cdots\frac{E_M[u_{k+1}]}{E_M[u_k]}$$
$$\leq \left(\frac{M[u_n]}{M[u_{n+1}]}\right)^{\frac{2}{p-1}}\left(\frac{M[u_{n-1}]}{M[u_n]}\right)^{\frac{2}{p-1}}\cdots\left(\frac{M[u_k]}{M[u_{k+1}]}\right)^{\frac{2}{p-1}}.$$

Therefore,

$$\frac{E_M[u_{n+1}]}{E_M[u_k]} \leq \left(\frac{M[u_k]}{M[u_{n+1}]}\right)^{\frac{2}{p-1}}.$$

Letting $n \to \infty$ yields

$$\liminf_{n\to\infty} \frac{E_1[u_n]}{E_M[u_k]} \leq (M[u_k])^{\frac{2}{p-1}} \leq 1.$$

□

We conclude with a proof of the theorem.

Proof. [Proof of Theorem 4.7] The proof follows from noting that (4.26) holds when $M[u_0] \leq 1$, and (4.26) holds trivially if $M[u_0] \geq 1$. Inequality (4.27) follows by looking at the iteration in Lemma 4.8 with sequence elements u_{n_k} from Theorem 1.2. □

5. Examples. In this section, we present a few numerical examples illustrating the algorithm.

5.1. 1D Examples. For a first example, we consider the following instance of (1.5)

$$\phi'' - \phi + |\phi|^2\phi = 0, \quad \phi(\pm X_{\max}) = 0, \tag{5.1}$$

for some $X_{\max} > 0$. The advantage of considering such a problem is that its solution can be expressed in terms of a Jacobi elliptic[1] function as,

$$\phi(x) = (1+\beta^2)\,\mathrm{cn}\left(\beta x; \tfrac{1}{2}(1+\beta^{-2})\right),$$

where $\beta > 0$ solves $\mathrm{cn}\left(\beta X_{\max}; \frac{1}{2}(1+\beta^{-2})\right) = 0$.

5.2. Profiles. We discretize (5.1) with piecewise linear finite elements on $N+1$ uniformly spaced mesh points in $(-X_{\max}, X_{\max})$, and we approximate the nonlinear term as

$$\left|\sum u_j\varphi_j\right|^{p-1}\left(\sum u_j\varphi_j\right) \approx \sum |u_j|^{p-1}u_j\varphi_j. \tag{5.2}$$

In this problem, we take $\gamma = \gamma_\star = p/(p-1)$. Throughout, $X_{\max} = 2$. As we seek a positive solution of (5.1), as an initial guess, we take

$$u_0 = (X_{\max} - x)(X_{\max} + x). \tag{5.3}$$

The profiles, obtained via the Petviashvilli iteration with different values of N, are plotted in Figure 5.1. All are in visual agreement with the exact solution. Turning

[1] We use the definition $\mathrm{cn} = \mathrm{cn}(x; m)$ rather than $\mathrm{cn} = \mathrm{cn}(x; k^2)$.

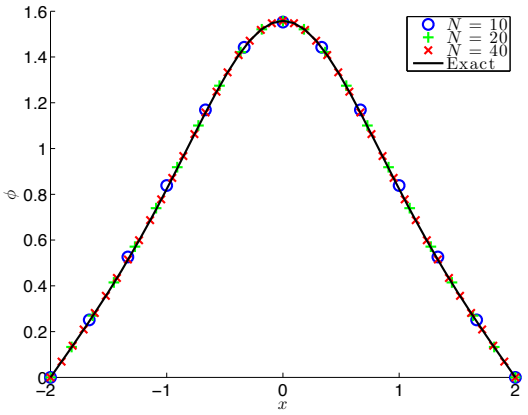


FIG. 5.1. *Solutions to* (5.1) *with* $X_{\max} = 2$ *at different resolutions. These are the profiles obtained after 100 iterations of the algorithm.*

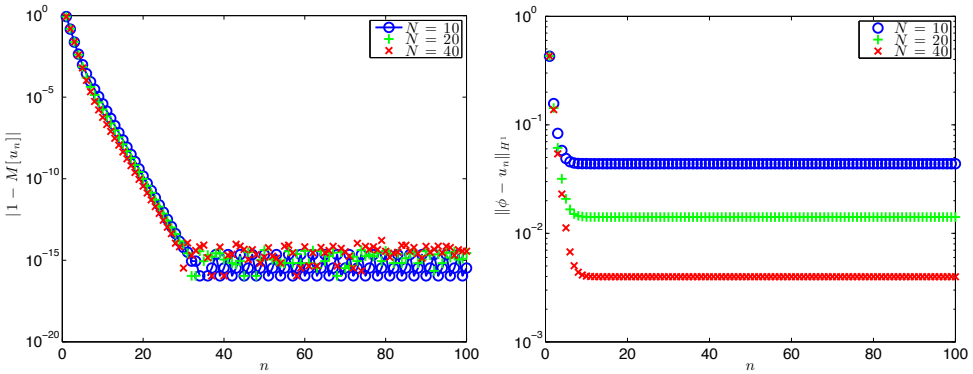
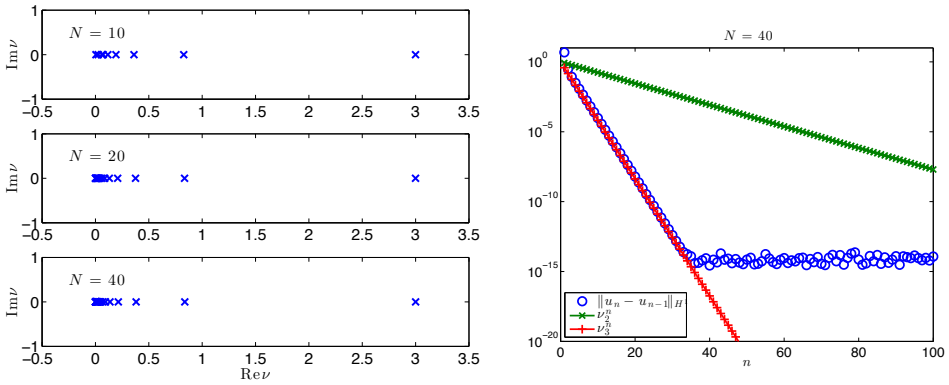


FIG. 5.2. *Convergence of the algorithm for* (5.1)*, measured in terms of* $|M[u_n] - 1|$ *and the* H^1 *error against the exact solution.*

to convergence, in Figure 5.2, we examine the H^1 error and the distance of $M[u_n]$ to 1. Several desirable properties are seen. First, as our analysis has been of the semi-discrete algorithm (without having introduced a mesh), we would hope to have mesh insensitivity; the convergence of $M[u_n]$ is relatively indifferent to N. Next, we see in the H^1 convergence figure that the error reaches a plateau. This is to be expected, as we must contend with both discretization and algorithmic error. We believe these plateaus reflect the error between the analytic solution and the discretized one, and the reduction of error with mesh refinement is consistent with this.

Finally, convergence Figure 5.2 indicates that, though we let the algorithm run for 100 iterations, we could have terminated after far fewer, perhaps 10-20 iterations, and obtained a high quality solution.

5.3. Spectral Analysis and Linear Convergence. Key to our linearized analysis was the spectral assumption that p was the only eigenvalue of $\mathcal{L}^{-1}(p\,|\phi|^{p-1})$ that was outside the unit disk, Assumption 4. In addition, Proposition 3.3 tells us that, in the case $\gamma = \gamma_\star$, the contraction mapping constant, θ, will be the largest



(a) (b)

FIG. 5.3. *On the left, we have the spectrum of the eigenvalue problem* (5.4) *with different numbers of mesh points. In all cases, there is a single eigenvalue at* $p = 3$*, and the next largest eigenvalue is near* $.84 < 1$*. On the right, we have successive differences, measured in the* H^1 *norm, of the iteration scheme. Note that while* $\mu_\star$ *is* $\nu_2 \approx .84$ *from Figure 5.3(a), the convergence rate follows* ν_3^n*, with* $\nu_3 \approx .38$*, the next largest eigenvalue.*

eigenvalue smaller than p.

Using the solution we have computed, we numerically solve the equivalent generalized eigenvalue problem

$$p\,|\phi|^{p-1}\,\psi = \nu\mathcal{L}\psi, \tag{5.4}$$

and find that this is indeed the case. The numerically computed spectrum for different values of N are plotted in Figure 5.3(a). As hoped for, the only eigenvalue in excess of one is $p = 3$, and the spectrum is nonnegative.

This begs the question as to whether or not, when u_n is sufficiently close to ϕ, the algorithm truly obeys (3.3). In Figure 5.3(b), we plot $\|u_{n+1} - u_n\|_{H^1}$, which, if we are sufficiently close to ϕ, should satisfy the contraction

$$\|u_{n+1} - u_n\|_{H^1} \leq \mu_\star \|u_n - u_{n-1}\|_{H^1}\,. \tag{5.5}$$

Recall that $\mu_\star$ is the largest eigenvalue beneath p associated with (5.4). We plot this difference in Figure 5.3(b). Note $\mu_\star = \nu_2 \approx .84$, but the successive error, $\|u_{n+1} - u_n\|_{H^1}$, does not follow ν_2^n. Instead, it follows ν_3^n, $\nu_3 \approx .38$ being the next smallest eigenvalue.

This can be understood in terms of symmetry. Problem (5.1) is a symmetric problem with even solution, the iteration scheme preserves symmetry, and the initial guess (5.3) is even. Thus, we are restricted to the closed subspace of even $H_0^1(-X_{\max}, X_{\max})$ functions. The eigenvalue, ν_2, corresponds to an odd eigenfunction, and thus plays no role.

5.4. Robustness to the Initial Condition. In the preceding example, our initial guess (5.3) is a highly informed choice; it is signed, smooth, and even. This begs the question of how the algorithm behaves when a poor guess is made. Let us try run the algorithm with a "rough" starting guess

$$u_0 = \sum_j c_j \varphi_j, \quad c_j \sim U(-1, 1), \tag{5.6}$$

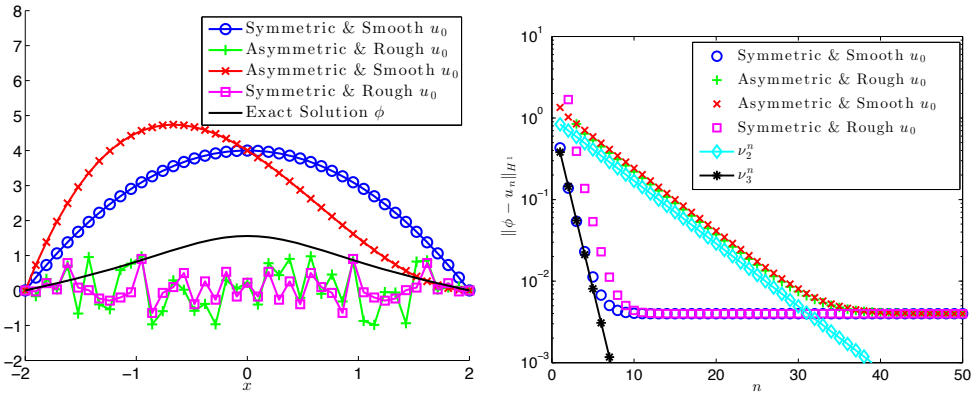


FIG. 5.4. *Initial profiles used to solve* (5.3) *and the convergence of the algorithm towards a solution. Symmetric initial conditions converge at a rate of* $\nu_3 < \nu_2$ *while asymmetric ones converge at this latter, slower rate.*

where φ_j are the hat function finite elements, and c_j are independent, identically distributed, uniform random variables. We also consider the asymmetric, but smooth, initial condition

$$u_0 = \tfrac{1}{2}(X_{\max} - x)^2(X_{\max} + x), \tag{5.7}$$

and the symmetrization of (5.6)

$$\frac{1}{2}\left(u_0^{\text{rough}}(x) + u_0^{\text{rough}}(-x)\right).$$

These initial guesses, along with the solution are shown in Figure 5.4(a). For all guesses, we obtain the solution, and as shown in Figure 5.4(b), the algorithm is relatively insensitive to the roughness of the data. Instead, it is the symmetry that dominates the problem. These computations reflect Theorem 1.2 and Corollary 1.3, which tell us that, generically, a subsequential limit exists, and if this limit is linearly stable, then the entire sequence converges to it.

5.5. 2D Examples with Radial Symmetry. Next, we consider solving the problem in 2D under a radial symmetry assumption. This reduces it to a 1D problem on $(0, R_{\max})$ with a Neumann boundary condition at the origin:

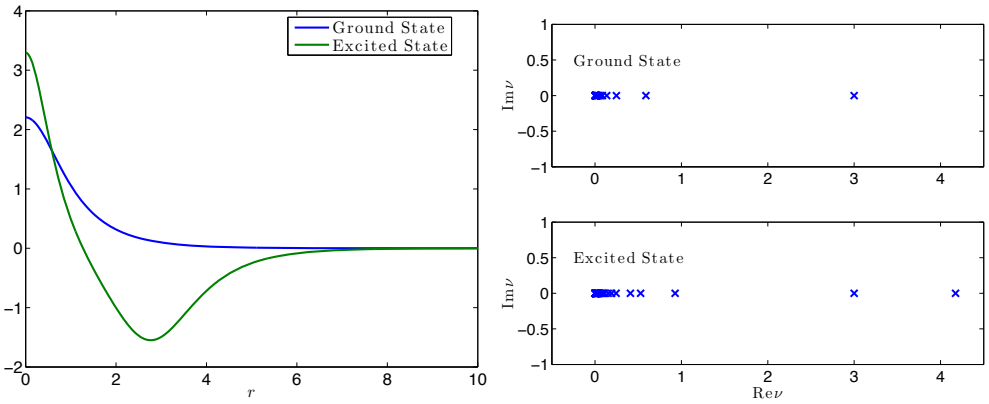
$$-\partial_r^2\phi - \tfrac{1}{r}\partial_r\phi + \phi - |\phi|^2\phi = 0, \quad \partial_r\phi|_{r=0} = \phi(R_{\max}) = 0. \tag{5.8}$$

Starting from the initial guess,

$$u_0(r) = {R_{\max}}^2 - r^2, \tag{5.9}$$

we compute the ground state using piecewise linear finite elements on the domain $(0, 25)$. With five hundred uniformly spaced elements in this interval, we obtain the ground state solution shown in Figure 5.5.

It is known that on the domain $(0, \infty)$, (5.8) has infinitely many real valued solutions with an arbitrary number of zero crossings [20]. And yet, no matter the initial condition u_0, the algorithm always appears to converge to a ground state. This begs the question of why. Here, we adapt our algorithm to compute an excited state



(a) (b)

FIG. 5.5. *The ground state and an excited state solution to* (5.8) *computed on the domain* $(0, 25)$*, along with the spectrum of* $\mathcal{L}^{-1}(p\,|\phi|^{p-1}\bullet)$ *for each state. Both have the unstable eigenvalue at* $p = 3$*, but the excited state has a second unstable eigenvalue.*

solution, and, *a posteriori*, we observe that it violates the spectral Assumption 4, introducing a linear instability.

Given $r_0 \in (0, R_{\max})$, let $\phi^{(0)}$ and $\phi^{(1)}$ solve the two boundary value problems

$$\begin{aligned} -\partial_r^2\phi^{(0)} - \tfrac{1}{r}\partial_r\phi^{(0)} + \phi^{(0)} - |\phi^{(0)}|^2\phi^{(0)} = 0, \quad 0 < r < r_0 \\ \partial_r\phi^{(0)}\Big|_{r=0} = \phi^{(0)}(r_0) = 0, \end{aligned} \tag{5.10}$$

$$\begin{aligned} -\partial_r^2\phi^{(1)} - \tfrac{1}{r}\partial_r\phi^{(1)} + \phi^{(1)} - |\phi^{(1)}|^2\phi^{(1)} = 0, \quad r_0 < r < R_{\max} \\ \phi^{(1)}(r_0) = \phi^{(1)}(R_{\max}) = 0. \end{aligned} \tag{5.11}$$

We then define the slope mismatch function as

$$F(r_0) = \partial_r\phi^{(0)}\Big|_{r=r_0} - \partial_r\phi^{(1)}\Big|_{r=r_0}. \tag{5.12}$$

Wrapping a root finding algorithm around our solvers, we compute the value of r_0 at which the slopes match, which yields the excited state plotted in Figure 5.5.

Using these computed solutions, we then compute the linearized spectrum plotted in Figure 5.5. The excited state has a second eigenvalue larger than one. Thus, it is linearly unstable with respect to Petviashvilli's method, and this is why it is not found directly. It remains to be studied why the root finding problem associated with (5.12) stabilizes the algorithm.

5.6. 2D Examples without Symmetry. Finally, we demonstrate the algorithm on a domain that cannot be reduced to 1D. This is computed using FEniCS [14]. The problem is studied using piecewise linear triangular elements with parameters $p = 3$ and $\gamma = \gamma_\star$.

Consider the problem on the isosceles right triangle inscribed in $[0, 1]^2$. Here, an unstructured mesh was generated using Triangle [19]. As an initial guess, we take

$$u_0 = \exp\left\{-50\left[(x - \tfrac{1}{4})^2 + (y - \tfrac{1}{4})^2\right]\right\}. \tag{5.13}$$

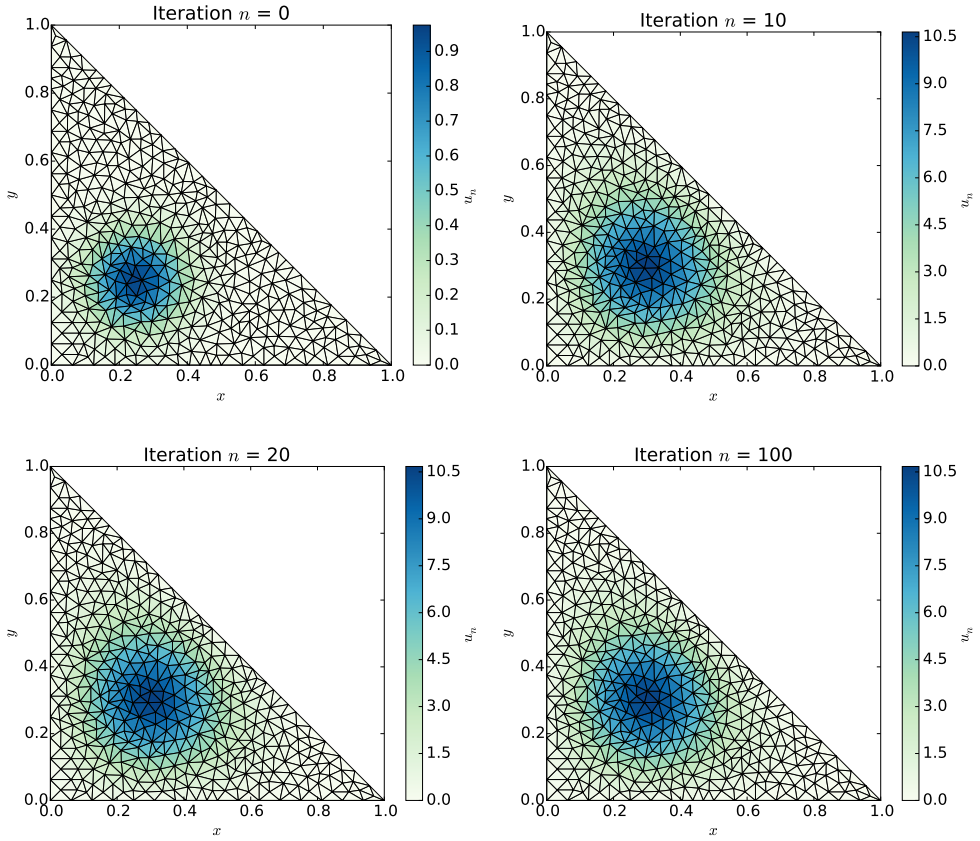


FIG. 5.6. *Solution to* (1.5) *on the triangular domain at several iterations. Note the change in scales between iterations.*

The solution, at several values of n, are displayed in Figure 5.6, and the diagnostics, $|M[u_n] - 1|$ and $\|u_{n+1} - u_n\|_{H^1}$ are shown in Figure 5.7. As in the 1D case, the algorithm rapidly enters the linear regime and returns the ground state despite our choice of initial condition.

6. Discussion. We have demonstrated and analyzed a computational algorithm for solving the Dirichlet problem for (1.5). Here, we remark on some of our results and highlight open problems.

Our local results were predicated on Assumption 4, and we have shown that, in some cases, it can be verified *a posteriori*. But the question remains as to whether or not it will hold generically for the ground state solution to the Dirichlet problem. For the problem on $\mathbb{R}^d$, more can been said. In [16], it is shown that the number of unstable directions of $(I - \Delta)^{-1}(p\,|\phi|^{p-1}\,\bullet)$ can be related to the number of negative eigenvalues of

$$\mathcal{H} = I - \Delta - p\,|\phi|^{p-1}\,\psi.$$

$\mathcal{H}$ is just the linearization of (1.3), and its spectrum is well characterized [20]. In the subcritical regime, $(p-1)d < 4$, $\mathcal{H}$ has a single negative eigenvalue which will

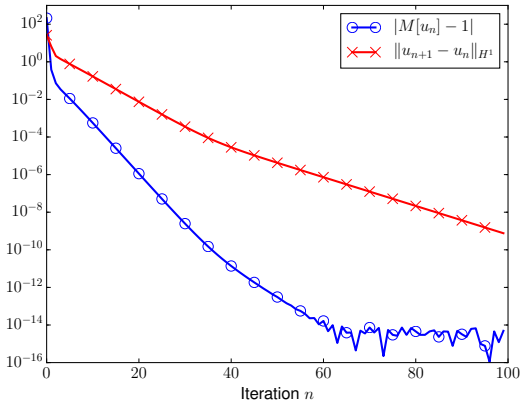


FIG. 5.7. *Diagnostics of the convergence of* $u_n \to \phi$ *when solving* (1.5) *on the triangular domain.*

correspond to the unstable eigenvalue p for $(I-\Delta)^{-1}(p\,|\phi|^{p-1}\,\bullet)$. $\mathcal{H}$ also has a kernel, $\nabla\phi$, which would correspond to a neutral eigenvalue of 1 in the iteration algorithm.

For the Dirichlet problem, $\nabla\phi$ is not in H_0^1, as it will fail to vanish at the boundary, so the neutral mode is eliminated. We conjecture that on sufficiently large and symmetric domains, the Dirichlet problem will inherit the same number of unstable eigenvalues as that of the problem on $\mathbb{R}^d$, but for small domains, or domains with significant geometry, we cannot say, *a priori*, what becomes the spectrum.

Our approach can be applied to simple generalizations of (1.5) such as

$$-\lambda\phi + \Delta\phi + |\phi|^{p-1}\,\phi = 0,$$

where λ is assumed larger than the first Dirichlet eigenvalue of the Laplacian on Ω. More significant generalizations would involve the inclusion of external potentials or symmetry breaking nonlinearities. This analysis might also be carried out for problems with other boundary conditions, such as Neumann or Robin.

The main outstanding problem remains to explain the experimentally observed generic convergence towards ground state solutions, even for data far from any solution. We have shown strong subsequential convergence, but we can only show that the sequence is Cauchy when the limiting solution satisfies particular spectral properties.

Another challenge is to consider the total error of the algorithm, as an approximation to the problem on $\mathbb{R}^d$. The total error could be decomposed as:

$$\underbrace{\left\|\phi - u_n^{(\Delta x,\Omega)}\right\|}_{\text{Total Error}} \le \underbrace{\left\|\phi - \phi^{(\Omega)}\right\|}_{\text{Modeling Error}} + \underbrace{\left\|\phi^{(\Omega)} - \phi^{(\Delta x,\Omega)}\right\|}_{\text{Discretization Error}} + \underbrace{\left\|\phi^{(\Delta x,\Omega)} - u_n^{(\Delta x,\Omega)}\right\|}_{\text{Algorithmic Error}}.$$

We expect that the truncation error will be most severe with the Dirichlet boundary condition, which is why Robin boundary conditions merit study. A particularly important case for such a complete analysis would be the radial case in dimension d. This is because investigations of soliton dynamics for (1.1) and (1.2) are frequently performed with radial symmetry. modelling

Acknowledgements. The authors are grateful for several helpful conversations with Svitlana Mayboroda. D.Olson was supported by the Department of Defense (DoD) through the National Defense Science and Engineering Graduate Fellowship

(NDSEG) Program. S.Shukla was supported by University of Minnesota UROP-11133. G.Simpson began this work under the support of the DOE DE-SC0002085 and the NSF PIRE OISE-0967140, and completed it under NSF DMS-1409018. D.Spirn was supported by NSF DMS-0955687.

REFERENCES

[1] M. J. Ablowitz and Z. H. Musslimani, *Spectral renormalization method for computing self-localized solutions to nonlinear systems*, Opt. Lett., 30 (2005), pp. 2140–2142.

[2] V. Adolfsson, *L^p-integrability of the second order derivatives of Green potentials in convex domains*, Pac. J. Math., 159 (1993), pp. 201–225.

[3] J. Álvarez and A. Duran, *Petviashvili type methods for traveling wave computations: I. Analysis of convergence*, J. Comput. Appl. Math., 266 (2014), pp. 39–51.

[4] M. Badiale and E. Serra, *Semilinear elliptic equations for beginners, existence results via the variational approach*, Springer, 2011.

[5] G. Baruch and G. Fibich, *Singular solutions of the L^2-supercritical biharmonic nonlinear Schrödinger equation*, Nonlinearity, 24 (2011), pp. 1843–1859.

[6] T. Cazenave, *An introduction to semilinear elliptic equations*, Federal University of Rio, Editora do IM-UFRJ, Rio de Janeiro, 2006. `https://www.ljll.math.upmc.fr/cazenave/77.pdf`.

[7] M. Chugunova and D. E. Pelinovsky, *Two-pulse solutions in the fifth-order KdV equation*, Discrete Cont. Dyn.-B, 8 (2007), pp. 773–800.

[8] L. Demanet and W. Schlag, *Numerical verification of a gap condition for a linearized nonlinear Schrödinger equation*, Nonlinearity, 19 (2006), pp. 829–852.

[9] S. Fromm, *Potential space estimates for green potentials in convex domains*, P. Am. Math. Soc., 119 (1993), pp. 225–233.

[10] D. Gilbarg and N. S. Trudinger, *Elliptic partial differential equations of second order*, Springer-Verlag, 2001.

[11] V. Hutson, J. S. Pym, and M. J. Cloud, *Applications of Functional Analysis and Operator Theory Analysis and Operator Theory*, Elsevier, second ed., 2005.

[12] T. I. Lakoba and J. Yang, *A generalized Petviashvili iteration method for scalar and vector Hamiltonian equations with arbitrary form of nonlinearity*, J. Comput. Phys., 226 (2007), pp. 1668–1692.

[13] ———, *A mode elimination technique to improve convergence of iteration methods for finding solitary waves*, J. Comput. Phys., 226 (2007), pp. 1693–1709.

[14] A. Logg, K.-A. Mardal, G. N. Wells, et al., *Automated Solution of Differential Equations by the Finite Element Method*, Springer, 2012.

[15] Z. H. Musslimani and J. Yang, *Self-trapping of light in a two-dimensional photonic lattice*, J. Opt. Soc. Am. B, 21 (2004), pp. 973–981.

[16] Dmitry E Pelinovsky and Yury A Stepanyants, *Convergence of Petviashvili's iteration method for numerical approximation of stationary solutions of nonlinear wave equations*, SIAM J. Numer. Anal., 42 (2004), pp. 1110–1127.

[17] V. I. Petviashvilli, *Equation of an extraordinary soliton*, Plasma Physics, 2 (1976).

[18] M. Reed and B. Simon, *Methods of Modern Mathematical Physics: Functional Analysis*, vol. 1, Academic Press, 1980.

[19] J. R. Shewchuk, *Triangle: Engineering a 2D Quality Mesh Generator and Delaunay Triangulator*, in Applied Computational Geometry: Towards Geometric Engineering, Ming C. Lin and Dinesh Manocha, eds., Springer-Verlag, 1996, pp. 203–222.

[20] C. Sulem and P.-L. Sulem, *The Nonlinear Schrödinger Equation: Self-Focusing and Wave Collapse*, Springer, 1999.

[21] J. Yang and T. I. Lakoba, *Universally-convergent squared-operator iteration methods for solitary waves in general nonlinear wave equations*, Stud. Appl. Math., 118 (2007), pp. 153–197.

[22] ———, *Accelerated imaginary-time evolution methods for the computation of solitary waves*, Stud. Appl. Math., 120 (2008), pp. 265–292.